applied sciences

MDPI

Article

Techno-Economic Analysis of the Peak Shifting Strategy Based on Time-of-Use Tariff for Cold Stores

Yanpeng Li [1], Chuang Wang [1,*], Zengqun Li [2], Dawei Ren [1,2], Ziwen Xing [1], Dawei Wu [2] and Huagen Wu [1]

1 School of Energy and Power Engineering, Xi'an Jiaotong University, Xi'an 710049, China
2 Moon Environment Technology Co., Ltd., Yantai 264000, China
* Correspondence: chuangwang@xjtu.edu.cn; Tel.: +86-132-8922-7655

Abstract: The energy consumption in the cold store is growing day by day, 70% of which is consumed by the refrigeration system. Meanwhile, a significant amount of electricity generated by power plants is wasted during off-peak periods. Demand-side management (DSM) provides a viable solution for addressing the problem of the time and space inconsistency between energy supply and consumption, hence improving overall system efficiency. In this paper, an artificial intelligence model is developed for accurate cooling load forecasting. On this basis, a peak shifting control strategy with two optional modes combining temperature setpoint control and operation mode control is then proposed to realize cost reductions. Taking a large-scale cold store as a case study, the cooling capacity supply and temperature variation within two typical working days are investigated to illustrate the feasibility and applicability of the strategy. Detailed thermodynamic and thermo-economic analyses of the proposed strategy are then carried out to demonstrate the control effect. The results show that both modes have good peaking performances and the average cost reduction rate of the two modes reaches 40% and 13.4%, respectively.

Keywords: cold store refrigeration system; peak shifting; LSTM prediction; intelligent control; energy-saving operation

check for updates

Citation: Li, Y.; Wang, C.; Li, Z.; Ren, D.; Xing, Z.; Wu, D.; Wu, H. Techno-Economic Analysis of the Peak Shifting Strategy Based on Time-of-Use Tariff for Cold Stores. *Appl. Sci.* **2023**, *13*, 11855. https://doi.org/10.3390/app132111855

Academic Editors: Luisa F. Cabeza and Sébastien Poncet

Received: 4 September 2023
Revised: 19 October 2023
Accepted: 26 October 2023
Published: 30 October 2023

1. Introduction

Economic development has stimulated people's demand for higher-quality and much healthier lives and has thus promoted the development of cold stores. In China, the energy consumption of large-scale cold stores is up to 91.3 kWh·m^{-3} [1,2], among which refrigeration systems account for about 70% [3]. Subject to the requirements of carbon peak and carbon neutralization, as well as the need for energy savings and emission reductions, the real-time optimization and energy management of large-scale cold stores is of great significance [4].

Thermal power plants, whose capacities are usually determined by peak demand, are still a main source of energy. Constrained by the stable operation requirements of the power supply equipment itself, the electricity generated during off-peak periods is wasted in enormous quantities. Demand-side management (DSM) is an important approach to handling the problem of time and space inconsistency from energy supply to consumption, as well as improve overall system efficiency [5,6]. As one of the DSM strategies, peak shifting refers to storing thermal energy during off-peak periods and releasing it when needed and has attracted increasing attention from researchers worldwide in the past decades. In general, there are three basic types of commonly adopted energy storage solutions, including thermal energy storage (TES), building thermal mass (BTM), and phase change material (PCM). A TES system is a reversible thermal energy storage device that is supposed to be applicable in DSM [7–10]. BTM utilizes the thermal energy storage capacity of building structures and furniture, that is, thermal inertia, to realize peak shifting [11,12]. The techno-economic feasibility of PCM as a cold energy storage medium has been illustrated by many studies [13–20]. High thermal inertia is the most critical property that can be used as an energy storage medium.

Studies conducted in the food and pharmaceutical industries have proven that short-term temperature overshoots or fluctuations have little effect on product quality [21–25]. Therefore, in the case of large-scale cold stores with high storage capacity, products can be used as the natural energy storage medium when peak shifting, and this is also an economic choice as it there is no additional equipment required [26]. Akerma et al. [23] conducted an experimental investigation on the application of demand response (DR) in a food cold store. The findings indicate that DR can relieve the strain on the power grid, and energy consumption can be reduced while maintaining product quality. To explore the application of the ice storage systems in libraries, Yau et al. [27] theoretically investigated the cost-saving effect under different storage strategies using TRNSYS software. It was revealed that all of the proposed strategies can achieve good economic results, with up to 60% cost savings. Similarly, a combined model, including the product finite element model and the cooling load model, was developed by Altwies et al. [24] for a cold store whose correction was accomplished through several days of experimental data. Furthermore, the corrected model was used to study the effect of load shifting, and it showed that a cost reduction of 37~53% could be realized without affecting product quality. Yin and Lee et al. [28,29] verified the effect of peak shifting under the strategy of setting the pre-cooling temperature and pre-cooling time from the perspective of experiments and simulations, respectively, and the results showed that the strategy can achieve an effective reduction in peak demand. To summarize, shifting cooling loads to achieve cost savings has become a popular research topic, and numerous studies have demonstrated its effectiveness. However, much of the existing research on peaking control strategies has focused on commercial buildings rather than cold stores, which would be more challenging because the temperature needs to be maintained within a suitable temperature range all day rather than that only during working hours. Furthermore, existing control strategies can be categorized into two main types. The first type, temperature setpoint control, aims to optimize the pre-cooling temperature to achieve maximum economic performance. The second aims to adjust the compressor operating mode at different times to achieve full or partial load shifting according to the time-of-use (TOU) tariff. However, the load level setting at different times is largely arbitrary, which can lead to insufficient or over-cooling and consequent energy wastage. As stressed by Sun et al. [30], developing a practical peak shifting strategy for real-time optimization to achieve further cost reduction or performance improvement is of great significance.

To combine the advantages of these two types of control strategies, this research innovatively proposes a peak shifting control strategy dedicated to cold stores which combines temperature setpoint control and compressor operating mode control to realize energy-saving operation. The cooling load of cold stores is strongly related to the weather conditions and thus has a remarkable periodicity in consecutive working days, which allows the LSTM algorithm to be used for its prediction. On the basis of the prediction results, two modes, A and B, are proposed to meet various control requirements in different cold stores. Actual operation data of a large-scale cold store are used to perform thermodynamic and thermo-economic analyses of the strategy to illustrate its validity. As an attempt to develop a peak shifting strategy in cold stores, this paper has achieved good peak shifting and cost-saving effects and thus can provide a reference for future research.

2. Refrigeration System

2.1. System Description

A large-scale cold store, whose products are used for long-term storage reserve, with ammonia as the refrigerant located in Henan, China, is studied to show the feasibility and effectiveness of the proposed strategy. The cold store covers an area of over 4800 m^2 with a storage capacity of over 7000 tons; its warehouse is shown in Figure 1a. The refrigeration system is simplified to a combination of 7 core components (Figure 1b) including the compressor unit, the centralized evaporative condenser, the centralized high-pressure ammonia storage, the throttle valve, the separator, the refrigerant pump, and the evaporator inside the warehouse. As the most essential refrigeration equipment, the main parameters of the compressor are shown in Table 1. The system contains two identical compressors operating in parallel that can be independently controlled, and both are equipped with capacity adjustment devices.

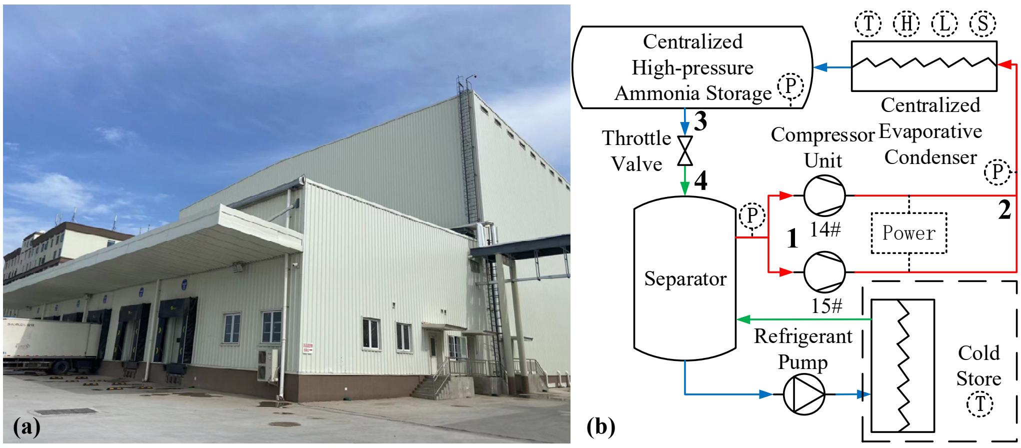

Figure 1. The refrigeration system of the cold store. (**a**) Overview of the warehouse; (**b**) Schematic diagram of the refrigeration system.

Table 1. Main parameters of the compressors.

Parameter	Compressor
Refrigerant	R717
Rated motor speed	2950 r·min^{-1}
Nominal cooling capacity	390 kW
Rated power	164 kW
Voltage/Frequency	380 V/3 N~50 Hz
Nominal condensing temperature	+36 °C
Nominal evaporating temperature	−28 °C

In the schematic, the direction of the line segment between components indicates the flow direction of the refrigerant in the pipeline, and the color indicates the state of the refrigerant (blue for the liquid, red for the gas, and green for the gas–liquid mixed phase).

With a separator as the medium, in which gas and liquid refrigerant exist simultaneously, a refrigeration circuit and a cooling circuit are connected, and thus energy exchange can be realized. The function of the refrigeration circuit is to generate low-temperature liquid refrigerant in the separator. The cooling circuit uses the generated refrigerant to provide cooling capacity to maintain the warehouse temperature within a reasonable range. The gas refrigerant in the separator is sucked and compressed by the compressor unit before being cooled in the evaporative condenser. After condensation, the refrigerant is stored in the centralized high-pressure ammonia storage and then throttled to the low-temperature fluid by the throttling valve to return to the separator to complete the refrigeration circuit. Being pumped into the evaporator in the warehouse, the liquid refrigerant evaporates to absorb heat and returns to the separator in the gas–liquid state. The two-phase refrigerant returning to the separator is separated again, among which the gas is used in the refrigeration circuit and the liquid re-enters to the cooling circuit.

2.2. Date Collection and Pre-Processing

The locations of the data collection points in this refrigeration system are identified by the dotted lines shown in Figure 1b. A total of 3 pressure sensors are included, measuring the pressure in the suction and discharge of the compressor unit and the centralized high-pressure ammonia storage. Neglecting the flow pressure loss, the suction and discharge pressures of the compressor unit can be regarded as the evaporating and condensing pressures. Several temperature sensors are installed at different sites within the warehouse, and the average temperature is used as the input for calculations. In practical cold stores, power sensors are rarely available due to their high price. The use of Electrical Specification Documents for electrical performance evaluation when there are no power sensors is recommended by Hinkelman et al. [31]. Hence, a constant power factor of 0.9 provided by the motor manufacturer is adopted for calculations. Environmental conditions such as outdoor temperature, humidity, light intensity, and wind speed are also collected to predict the cooling load. The main parameters of the data acquisition system used in this paper are shown in Table 2. To evaluate the accuracy of the collected data, the uncertainty can be calculated by the following equation series (Equations (1)–(3)), where Y is a function with vector x as a variable [32,33]. Accordingly, the maximum uncertainty of the cooling capacity is 1.02%.

$$Y = f(x_1, x_2, \cdots, x_n) \tag{1}$$

$$u_Y = \sqrt{\sum_{i=1}^{n} \left(\frac{\partial Y}{\partial x_i}\right)^2 u_i^2} \tag{2}$$

$$\frac{u_Y}{Y} = \sqrt{\sum_{i=1}^{n} \left(\frac{\partial Y}{\partial x_i} \cdot \frac{u_i}{y}\right)^2} \tag{3}$$

Table 2. Data collection system configuration.

Signal Type	Location	Range	Precision
Pressure	High-pressure side Low-pressure side	0~2.5 MPa 0~0.6 MPa	3‰ 3‰
Temperature	Environment Inside warehouse	−20~60 °C −50~100 °C	0.5 0.2
Humidity	Environment	0~1	2.5%
Current	Compressor	0~800 A	1%

Subject to sensor accuracy as well as refrigeration system characteristics, the directly collected data tend to have a high degree of volatility and mutability. In addition, with the purpose of limiting the cost of sensors for the cold store, some key parameters (e.g., cooling load) are not available. Hence, data preprocessing is of great importance. In this paper, a filtering algorithm was used to perform noise reduction of the raw data, and a thermodynamic model was established (see Section 3.2) to realize cooling load data supplementation. Finally, a representative data set could be obtained.

The filtering method used in this paper is the wavelet noise reduction algorithm, whose basic idea is to achieve noise removal based on the intensity distribution characteristics of the wavelet decomposition coefficients of the noise and signal in different frequency bands [34,35]. Compared with other algorithms, the wavelet noise reduction algorithm has a higher model recognition rate and is particularly effective in denoising time-varying and abruptly changing signals. To ensure the reliability of the calculation, all raw data generated by the acquisition needs to be filtered. A comparison of the before and after filtering effect of the compressor's suction and discharge pressure is shown in Figure 2, where it can be seen that some steep rises or drops that do not conform to common sense can be removed well.

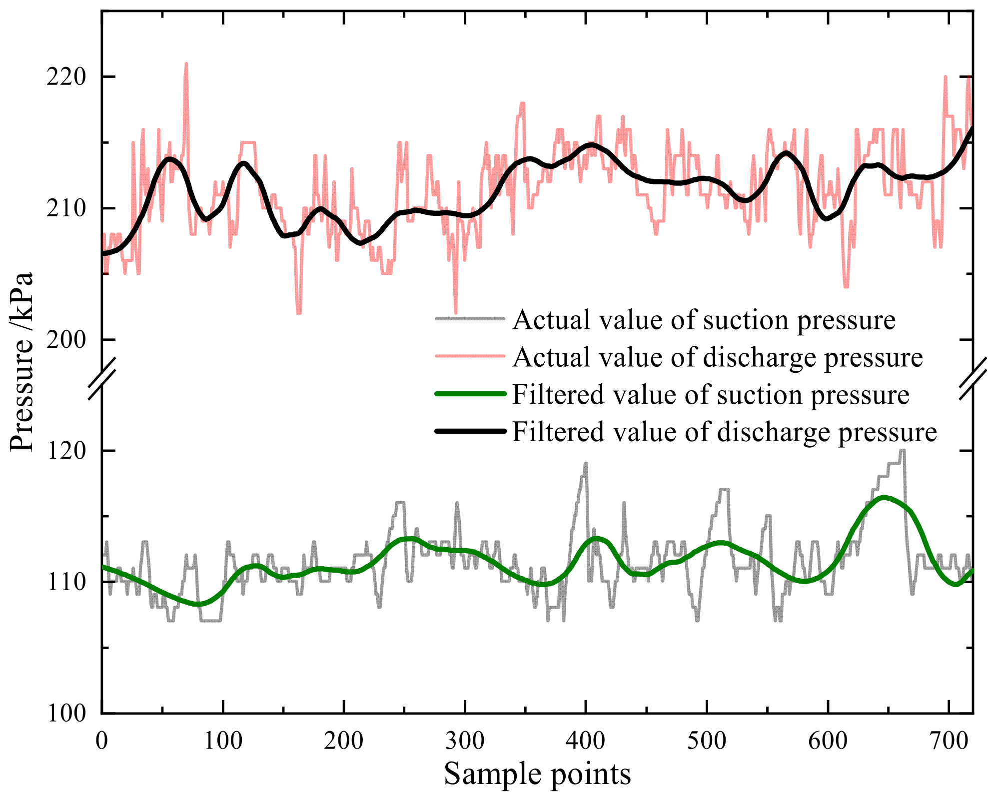

Figure 2. Comparison of before and after suction/discharge pressure filtering.

3. Methodology

3.1. Peak Shifting Calculation Flow

The peak shifting strategy is mainly based on the TOU tariff, where the operation of the compressors is shifted from peak to off-peak periods, resulting in cost savings. As shown in Table 3, the 24 h is divided into five periods, with a total of three types including peak, flat, and valley periods based on the electricity consumption situation. Since there are two separate peak and flat periods, this paper distinguishes them by 1# and 2#. The valley period is 0–8 a.m., during which the average ambient temperature tends to be much lower and the condensing pressure of the compressor unit can be further reduced, thus increasing the efficiency of the compressor unit.

Table 3. Time-of-use tariff.

Time (*h*)	**0~8**	**8~12**	**12~18**	**18~22**	**22~24**
Type	Valley	Peak_1#	Flat_1#	Peak_2#	Flat_2#
Price (CNY/*kWh*)	0.358	1.061	0.686	1.061	0.686

Detailed calculation flow is shown in Figure 3. The collected historical operation data need to be pre-processed first, and are then used as the input for the cooling load prediction in the LSTM algorithm. Based on the prediction results, two different operation modes are proposed to be selected according to practical production, where Mode A aims at complete load shifting while Mode B is a load-balancing strategy. Both modes combine the compressor operation mode control with the temperature setpoint control, thus offering the possibility to avoid overshooting the warehouse temperature.

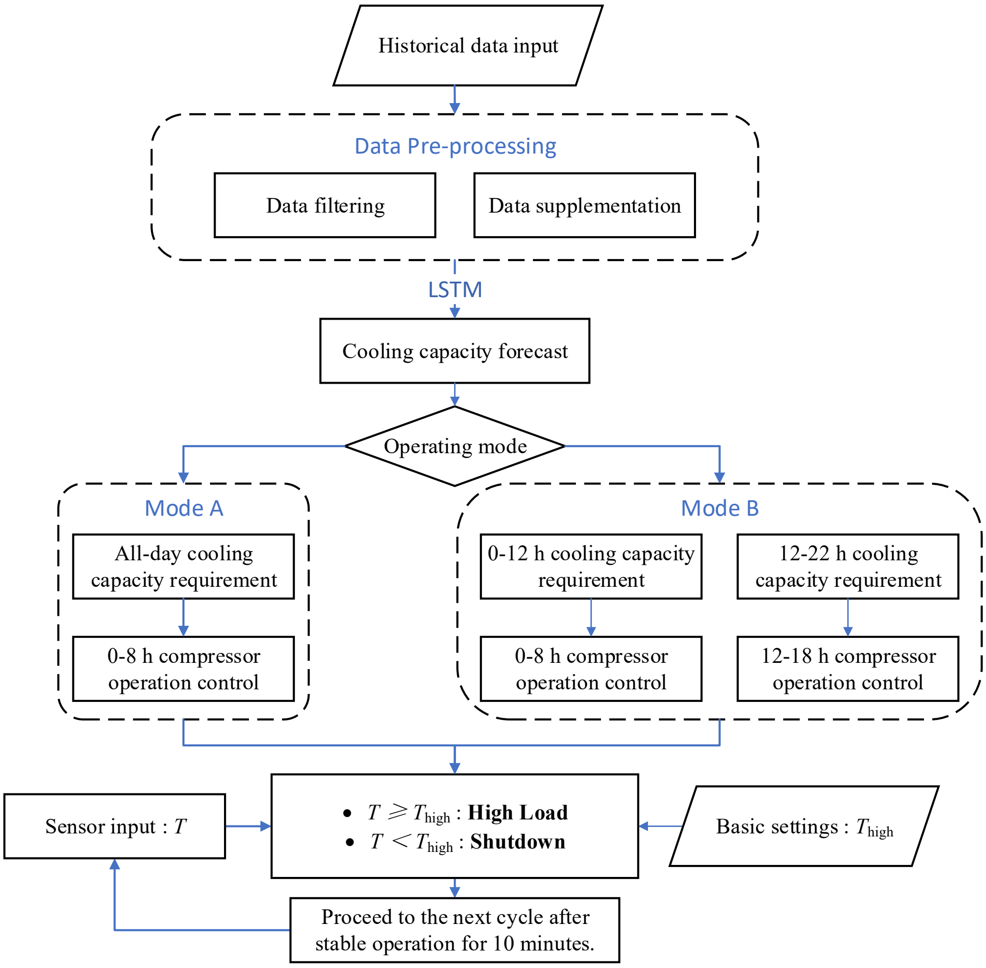

Figure 3. Detailed calculation flow of the peak shifting strategy.

From the point of view of the compressor properties, a low load will result in low adiabatic efficiency. This paper provides three efficient operation patterns for the compressor unit based on expert experience, corresponding to low, medium, and high load cases, as shown in Table 4. The load setting value is expressed as the sum of two numbers, representing the load of the first and second compressors, respectively.

Table 4. Compressor operation pattern under different loads.

Operation Pattern	Low Load	Medium Load	High Load
Load Calculation	<100%	100~150%	>150%
Load Setting	100% + 0%	75% + 75%	100% + 100%

3.2. Thermodynamic Model

To supplement the missing cooling load, a thermodynamic model of the refrigeration system is developed in this paper. Generally speaking, the modeling process should start by considering three fundamental conservation relations, including the continuity equation, the momentum equation, and the energy equation. The flow of the refrigerant in the pipeline is relatively smooth and therefore can be seen as a steady flow state, and the pressure drop is negligible, which means the continuity equation and the momentum equation naturally hold. Hence, only the energy equation needs to be considered while modeling. The positions of the key points in the refrigeration cycle are tagged as 1, 2, 3, and 4 in Figure 1b. Points 1 and 2 represent the suction and the discharge state of the compressor unit. Point 3 represents the state before throttling, and point 4 represents the state before evaporation. By quantitatively determining the thermodynamic state of the refrigerant at the import and export of each component, the enthalpy changes during each working process can be calculated [36].

The compression process can be simplified as an isentropic process whose isentropic compression power is given by Equation (4). The isentropic efficiency is introduced to evaluate the imperfection of the compression process. In this paper, the efficiency is defined as the ratio of the isentropic compression power to the input power of the drive motor, determined by Equation (5). According to experience, the isentropic efficiency of the compressor is strongly related to the pressure ratio [36]. In this paper, the efficiency is fitted based on the actual experimental data of the compressor. The fitting formula of the efficiency is shown in Equation (6):

$$P_{\mathrm{is,com}} = m \cdot (h_{2,\mathrm{is}} - h_1) \tag{4}$$

$$P_{\mathrm{com}} = m \cdot (h_{2,\mathrm{is}} - h_1)/\eta_{\mathrm{is}} \tag{5}$$

$$\eta_{is} = -0.0015 \cdot \varepsilon^2 + 0.0044 \cdot \varepsilon + 0.7515 \tag{6}$$

The evaporation process can be regarded as an isobaric process. The amount of heat exchange is given by Equation (7). The throttling process is irreversible, while the enthalpy of the inlet and the outlet are equal (Equation (8)).

$$Q_{\mathrm{eva}} = m \cdot (h_1 - h_4) \tag{7}$$

$$h_3 = h_4 \tag{8}$$

By associating Equations (5)–(8), the relationship between cooling capacity and the input power of the drive motor can be expressed as Equation (9). Due to the existence of the centralized high-pressure ammonia storage and the separator, the refrigerant steam quality at the termination of condensation and the beginning of compression is 0 and 1 respectively. As shown in Equations (10)–(12), the key enthalpies in Equation (9) can be determined quantitatively by invoking the CoolProp property library [37]. In summary, the cooling capacity can be determined as the input power of the drive motor and its suction and discharge pressure are determined.

$$Q_{\mathrm{eva}} = P_{\mathrm{com}} \cdot \eta_{\mathrm{is}} \cdot (h_1 - h_3)/(h_{2,\mathrm{is}} - h_1) \tag{9}$$

$$[h_1, s_1] = f(p = p_{evp}, q = 1) \tag{10}$$

$$h_{2,\mathrm{is}} = f(p = p_{con}, s = s_1) \tag{11}$$

$$h_3 = f(p = p_{con}, q = 0) \tag{12}$$

3.3. LSTM Model

To solve the problem of gradient disappearance in recurrent neural networks (RNNs), Hochreiter et al. [38] proposed a long short-term memory neural network (LSTM) capable of automatically learning information over a period of time in the past. LSTM increases the storage capacity of the loop cell by introducing 'gates' into the repetition module, including input gates, forgetting gates, and output gates. As a modified version of an RNN, LSTM classifies repetitive and periodic patterns in the data into long-term or short-term cycles and uses them as the output. Figure 4 illustrates the structure of the repetition module in which the amount of forgetting and memory information is regulated by the gates.

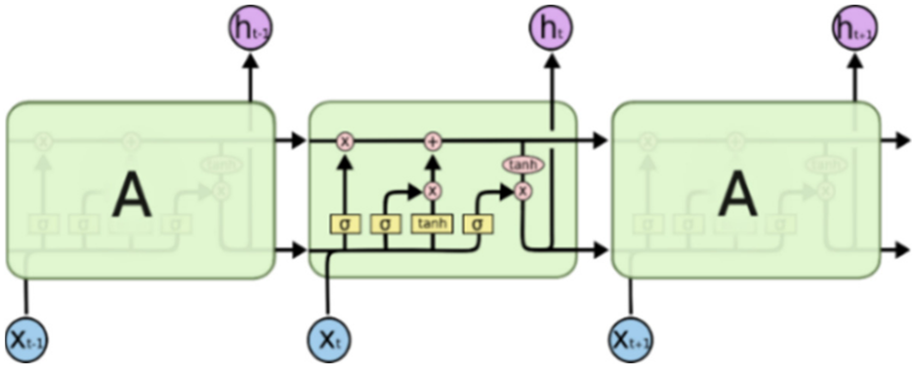

Figure 4. Structure of the repetition module in the LSTM algorithm.

The LSTM model's iterative formula is displayed in Equations (13)–(18) with initial values of $C_0 = 0$ and $h_0 = 0$, where b, W, and U represent the bias vector, weight connection matrix to the input, and weight connection matrix to hidden layers, respectively. And i, f, and o denote the input, forgetting, and output. The cell output vector is calculated as h_t.

$$i_t = \sigma(W_i x_t + U_i h_{t-1} + b_i) \tag{13}$$

$$f_t = \sigma\left(W_f x_t + U_f h_{t-1} + b_f\right) \tag{14}$$

$$o_t = \sigma(W_O x_t + U_O h_{t-1} + b_O) \tag{15}$$

$$\widetilde{C}_t = \tan(W_c x_t + U_o h_{t-1} + b_c) \tag{16}$$

$$C_t = f_t \otimes C_{t-1} + i_t \otimes \widetilde{C}_t \tag{17}$$

$$h_t = o_t \otimes \tan(C_t) \tag{18}$$

The cooling load of cold stores has significant periodicity, and thus the LSTM algorithm is well-suited for cooling load prediction. The environmental conditions (dry bulb temperature, relative humidity, wind speed, light intensity), the temperature of the warehouse, and the cooling load from the previous several days are used as model inputs in this paper. The scope of this research is the development of novel peak shifting strategies with the cooling load forecasts acting as the necessary pre-work. Therefore, in this research, the MATLAB toolbox is utilized directly to optimize the hyperparameters of the LSTM model rather than adopting new approaches.

3.4. System Simulation Approach

Two optional modes A and B are proposed in this paper for selection in practical production. The specific control principles for the two modes are as follows:

- Mode A: All-day cooling load needs to be shifted to the valley period and the compressor unit should maintain shutdown as much as possible in other periods. The operation mode during the valley period is set directly through the average load calculation result. Temperature set point control is adopted in off-valley periods, which means the unit shuts down before the temperature exceeds the upper limit and operates at high load when it does.
- Mode B: The cooling load of the whole day is divided into multiple intervals according to the TOU tariff and thus is met separately. The operation mode control is adopted in the valley as well as the flat_1# period. The compressor unit should both meet the cooling load of the above two periods and charge the storage to meet the demand from

the peak_1# and peak_2# periods. Similar to Mode A, temperature set point control is adopted in other periods.

The upper temperature limit can usually be determined by the storage requirements of the products, and it is set as −18 °C in this paper [21,22]. To compare the advantages and disadvantages of the above two modes, it is essential to analyze the trends of key parameters such as warehouse temperature, cooling capacity, and operation cost. Therefore, it is necessary to establish a simulation algorithm to analyze the control effect taking several actual working days as a case study. When the optimized temperature at the previous moment i is known to be $T_{\text{opti},i}$, the temperature at the following moment ($T_{\text{opti},i+1}$) can be calculated as Equation (19). $Q_{\text{ori},i}$ and $Q_{\text{opti},i}$ indicate the cooling capacity supply before and after peak shifting, respectively, whose difference is given in Equation (20).

$$T_{\text{opti},i+1} = T_{\text{opti},i} + \left(Q_{\text{opti},i} - Q_{\text{dis,opti},i}/c \cdot M\right) \tag{19}$$

$$\Delta Q_i = Q_{\text{opti},i} - Q_{\text{ori},i} \tag{20}$$

Similar to Equation (19), the relationship between the original temperature at adjacent moments can be expressed in Equation (21).

$$T_{\text{ori},i+1} = T_{\text{ori},i} + (Q_{\text{ori},i} - Q_{\text{dis,ori},i}/c \cdot M) \tag{21}$$

For the cold store discussed in this paper, the dissipation at the building envelope is positively correlated with the temperature difference between the inside and outside. Owing to the large reserve of products, the change in the warehouse temperature is very limited before and after peak shifting. Consequently, the cooling dissipation can be approximated as unchanged in the simulation calculation (Equation (22)). The recurrence relation for the optimized temperature can be determined by associating Equations (19)–(22), as shown in Equation (23). As the initial value, its temperature should be equal at the beginning moment when the control strategy is introduced (Equation (24)). In this research, the product in the cold store is mainly pork, and the specific heat capacity is given in Equation (25) [39].

$$Q_{\text{dis,opti},i} = Q_{\text{dis,ori},i} \tag{22}$$

$$T_{\text{opti},i+1} = T_{\text{opti},i} + T_{\text{ori},i+1} - T_{\text{ori},i} + (\Delta Q_i/c \cdot M) \tag{23}$$

$$T_{\text{opti},1} = T_{\text{ori},1} \tag{24}$$

$$c = 0.00286 \cdot T^2 + 0.1826 \cdot T + 5.83 \tag{25}$$

Analyzing the control effect of the strategy, it is worthwhile to compare the trends of the cooling capacity and the operation cost of the system. The cooling capacity provided by the system during operation can be calculated as Equation (26). The operation cost is dominated by the consumed electrical power of the compressor unit, so it can be formulated as Equation (27). Furthermore, the cost reduction rate is used to measure the economic effect before and after peak shifting (Equation (28)).

$$Cooling\ Capacity = \sum_{i=1}^{n} Q_{\text{eva}} \cdot \Delta t_i \tag{26}$$

$$COST = \sum_{i=1}^{n} EP_i \cdot P_{\text{com}} \cdot \Delta t_i \tag{27}$$

$$Cost\ Reduction\ Rate = 1 - \left(COST_{\text{opti}}/COST_{\text{ori}}\right) \tag{28}$$

4. Results and Discussion

In this study, the cyclical variation pattern of the cooling load in the previous several days is identified and that of the following day is predicted by LSTM. Based on the prediction results, the trends in cooling capacity supply and temperature changes before and after the adoption of the peak shifting strategy for a typical day are analyzed. A total of five consecutive working days are taken as a case study to illustrate the peak shifting effect and economics of the strategy.

4.1. LSTM Prediction Effect Analysis

In this paper, data from 10 consecutive working days are collected to validate the proposed method. The operation data are divided into two parts, the former 5 days is used for model training and pattern recognition and the latter 5 days for verifying the model prediction effect. The prediction results are shown in Figure 5, whose horizontal axis represents different working days (separated by short green lines) and the vertical axis represents the cooling capacity. It can obviously be seen that the cooling load in consecutive working days shows a strong periodic trend. A brief peak in the cooling load exists each day at 8–10 a.m., and this is mainly because it is the start of work. In addition, the cooling load is relatively stable throughout the day, and normally only one compressor is on. Analyzing the prediction results, it can be found that the predicted values of the cooling load match well with the test values. When dealing with longer periods, the model allows for continuous updating and iterating with the latest historical data, thereby guaranteeing prediction accuracy.

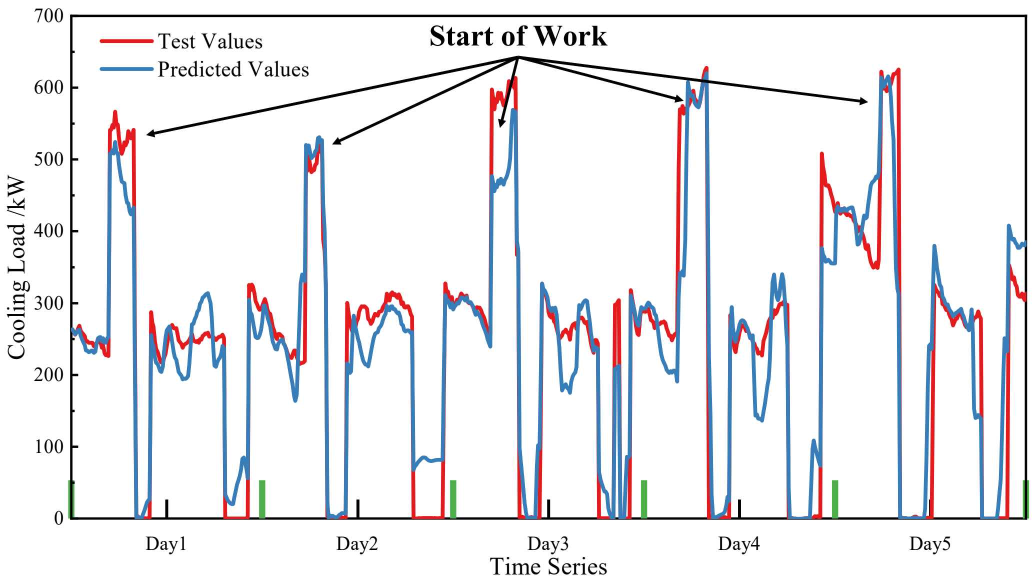

Figure 5. Comparison of the test and prediction cooling load over 5 working days (separated by short green lines).

The errors between the test and predicted values of the cooling load are shown in Figure 6, where 65% of the predicted cold load results can converge within the 20% error line with the R^2 of 0.8791. It is important to note that when adopting a peak shifting strategy, accurate time-to-time prediction is not necessary, and total load forecast is more important. From this point of view, the prediction accuracy is sufficient for peak shifting, and the LSTM algorithm is suitable for cooling load forecasting of cold stores.

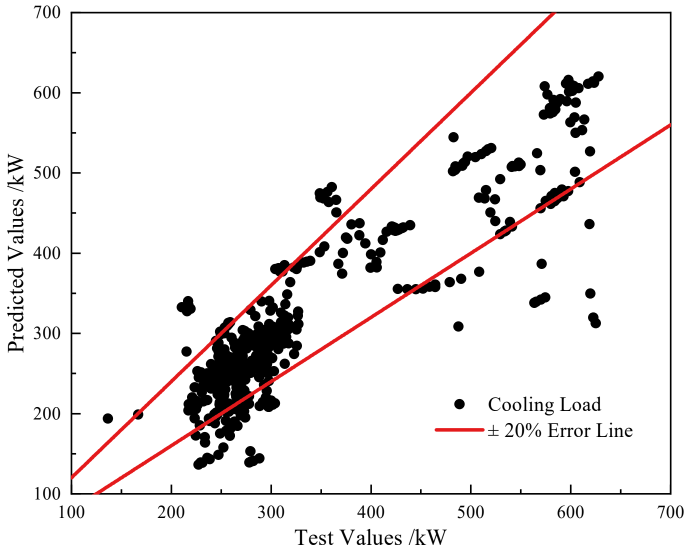

Figure 6. Errors between the test and predicted values.

4.2. Comparison of Control Effects

Figure 7 shows the comparison of cooling capacity supply between the original mode, Mode A, and Mode B on the first and third days. The solid black line represents the original mode, while the red and blue dashed lines represent Mode A and B, respectively. The cooling load of the cold stores will change chaotically and rapidly with the external environment, production conditions, etc. Under the original mode, the compressor unit runs at a low load for a long time, and this load may fluctuate with the cooling load, bringing additional energy waste and cost increases. The peak shifting results suggest that the compressor unit only operates during the valley period in Mode A and only in the valley and flat_1# periods in Mode B. Based on the reliable prediction of the cooling load, the operation of the compressor unit is switched to a high load and short time, enhancing the stability. By charging the storage during off-peak hours, the temperature of the warehouse can always be maintained within the appropriate range, so that no additional start-up of the compressor unit is required in both modes. It should be mentioned that while Mode A allows for complete shifting, it requires a larger capacity of the compressor unit, which may result in a potential initial cost increment. As a load-balancing solution, Mode B shifts the load to multiple suitable periods, which is also applicable to cases with a small unit capacity.

The variation in the warehouse temperature on the first and third days is shown in Figure 8. Basically, the trends before and after optimization are similar, but most of the time, the optimized temperature is slightly lower than the original one. For Mode A, its warehouse temperature reaches its lowest point around 6–8 a.m. and rises slowly during the rest of the day. The temperature of Mode B is in between the original mode and Mode A during the valley period. The temperature curves of the two modes overlap at around 17:00 but still remain below the original mode. At the end of the day, the temperature of the two modes returns to a similar level to the original one. From the perspective of operation safety, the temperature fluctuations in the cold store are another important indicator of an optimization strategy. Mode A results in greater temperature fluctuations than Mode B. The maximum temperature difference of Mode A in two days was 0.35 °C and 0.38 °C, while that of Mode B was 0.18 °C and 0.20 °C which is only about half of that of Mode A, based on the original temperature curve. Objectively speaking, temperature fluctuations in both modes are quite limited, and thus, the dissipation before and after the adoption of the peak shifting strategy can be approximated to be identical, as mentioned earlier. This is mainly due to the large thermal inertia of the cold store, which can keep the core temperature of the product relatively stable when external factors change temporarily [23,24].

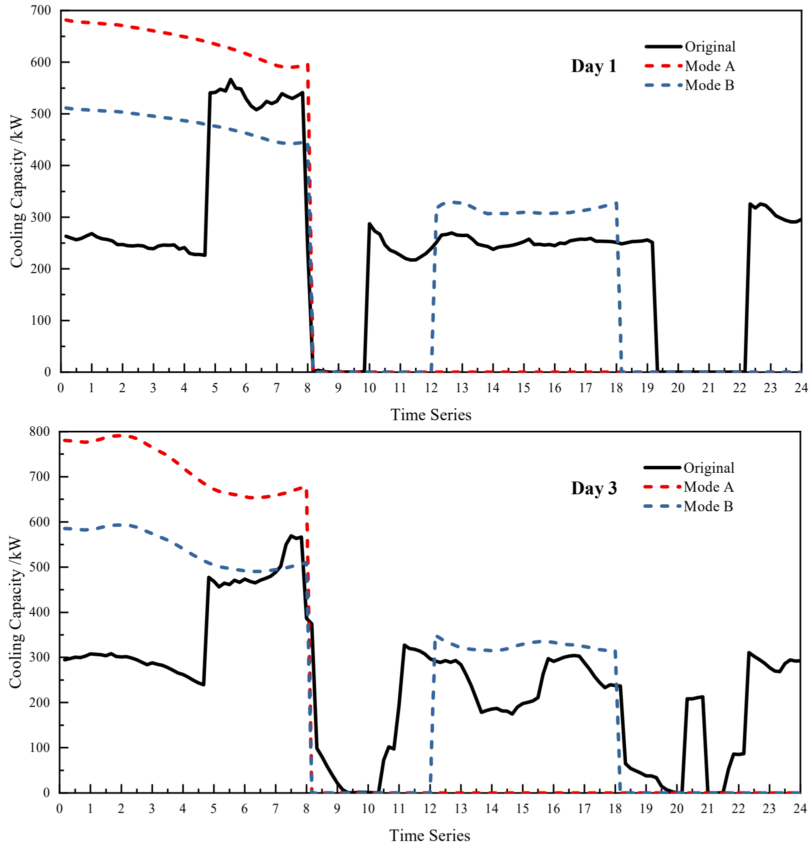

Figure 7. Comparison of the cooling capacity on two representative days.

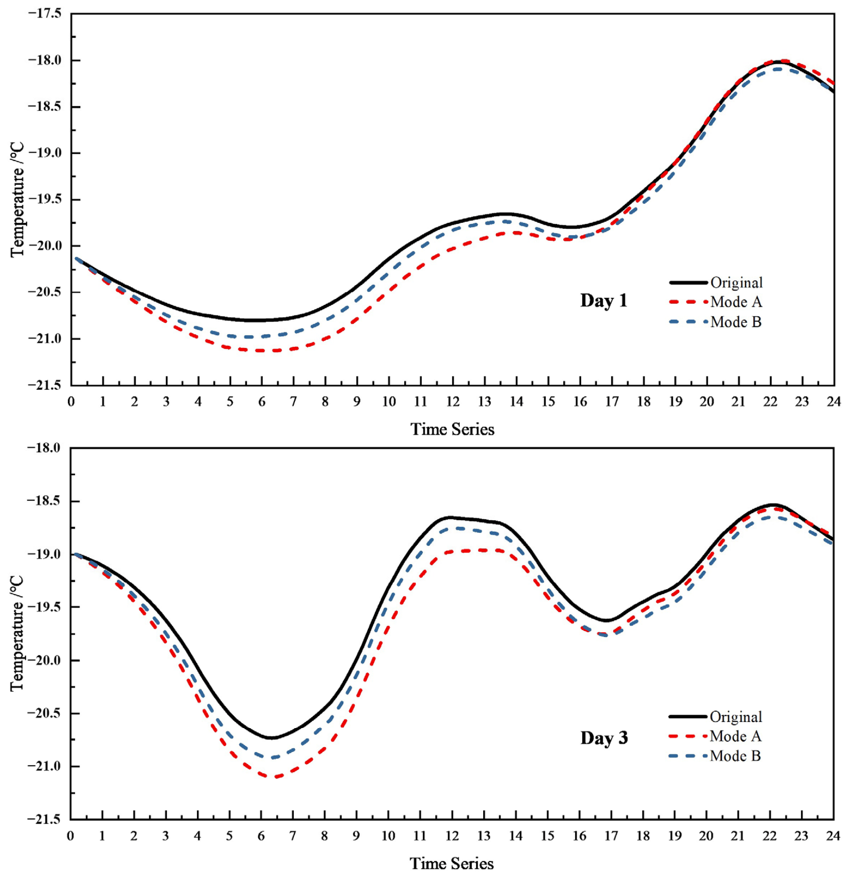

Figure 8. Comparison of the warehouse temperature on two representative days.

4.3. Analysis of Control Effects

The comparison of the cooling capacity before and after peak shifting is shown in Figure 9, where red, blue, and green represent the ratio of the cooling capacity provided in the peak, flat, and valley periods to the total amount of the day, respectively. The cooling capacity of the peak period accounts for 3~14% and the valley period accounts for only about half in the original mode. Mode A achieves complete shifting, and the cooling load is met in the valley period. The cooling capacity ratio of the valley period in Mode B has increased by about 15% on average, while that of the flat period remains almost the same as before. To sum up, both modes can achieve a good peak shifting effect.

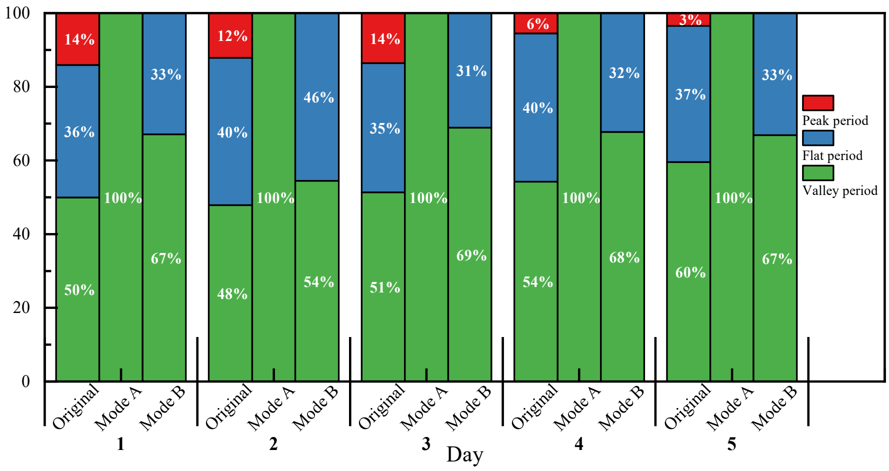

Figure 9. Effect of cooling capacity shifting.

The variation in the operating cost for 5 days is shown in Figure 10, in which the bars represent the cost and the lines indicate the cost reduction rate. Mode A is a more aggressive mode with an average cost reduction of about 40%. As a comparison, the average cost reduction rate of Mode B is only 13.4%. The cost reduction rate of both modes suffers a significant decrease on day 5 because the economy of the peaking strategy is mainly due to load shifting of the peak period while the cooling capacity of the peak period accounts for only 3% out of the total amount. In general, the strategy proposed in this paper can achieve a satisfactory reduction in operation costs without requiring changes in the physical structure of the system.

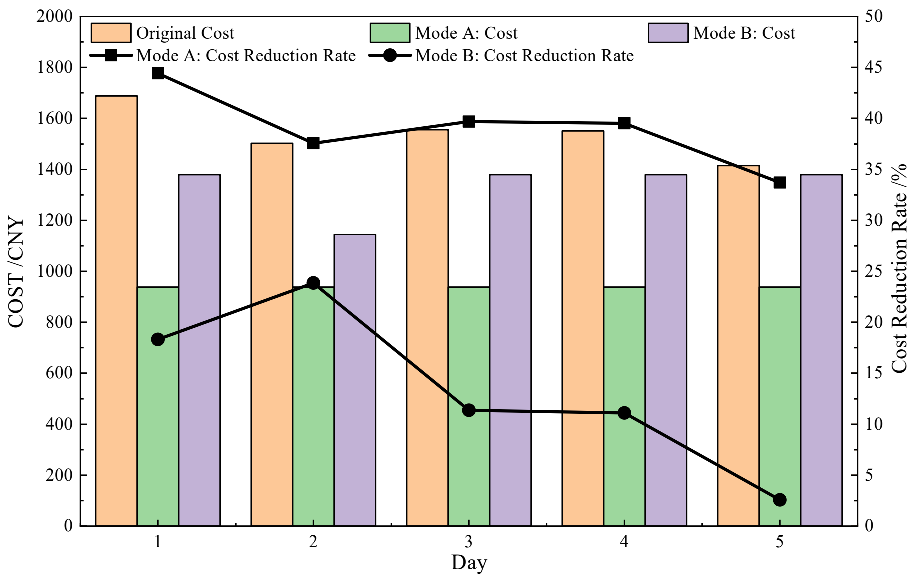

Figure 10. Economy comparison of peak shifting strategy.

5. Conclusions

In this paper, an artificial intelligence model for cooling load forecasting is developed using the LSTM algorithm at the first step and its reliability is illustrated. Based on the TOU tariff, a peak shifting control strategy with two optional modes which combine temperature setpoint control and operation mode control is then proposed to realize peak shifting as well as cost reductions. With the proposed strategy, the feasibility and applicability are evaluated by taking the actual operating data of five consecutive working days. Finally, the peak shifting effect and economy of the proposed strategy are demonstrated by comparing the ratio of the cooling capacity provided in different periods and the cost reduction rate. The detailed conclusions are as follows:

(1) The cooling load of the cold store has a significant periodicity during continuous working days, and therefore LSTM is suitable for load prediction. The results are of good accuracy and have engineering practicality.
(2) Mode A is a complete shifting strategy, which means the entire day's cooling load is met during the valley period. As a consequence, this mode offers a better economy, with an average cost reduction rate of approximately 40%. Nevertheless, this mode may result in larger temperature fluctuations and require a higher capacity of the compressor unit which brings much more initial investment.
(3) Mode B is a load-balancing strategy, which means the cooling load throughout the day is assigned to multiple appropriate periods to be met. Compared to Mode A, the average cost reduction rate for this mode is only 13.4%. However, this model causes smaller temperature fluctuations and does not require a higher capacity of the compressor unit.

Author Contributions: Conceptualization, C.W. and Z.X.; Data curation, D.R. and D.W.; Formal analysis, D.W.; Investigation, Y.L. and C.W.; Methodology, Z.L. and H.W.; Software, Y.L.; Supervision, Z.L. and Z.X.; Validation, D.R.; Writing—original draft, Y.L.; Writing—review and editing, C.W. All authors have read and agreed to the published version of the manuscript.

Funding: This research was funded by the National Natural Science Foundation of China, grant number 51976148. The authors gratefully acknowledge the financial support from the China Scholarship Council (No. 202306280272).

Institutional Review Board Statement: Not applicable.

Informed Consent Statement: Not applicable.

Data Availability Statement: The data that support the findings of this study are not available for privacy reasons.

Conflicts of Interest: The authors declare no conflict of interest.

Abbreviation:

Nomenclature
Symbols

T	temperature (°C)	c	specific heat capacity ($J{\cdot}kg^{-1}{\cdot}°C^{-1}$)
Δt	time step (s)	W	weight connection matrix to the input
P	power (kW)	U	weight connection matrix to hidden layers
p	pressure (kPa)	σ	sigmoid activation function
h	enthalpy ($J{\cdot}kg^{-1}$)	b	bias vector
s	entropy ($J{\cdot}kg^{-1}{\cdot}K^{-1}$)	$\widetilde{C}$	temporary state layer
η	efficiency	C	cell state vector

ε	pressure ratio	h	cell output vector
m	mass flow rate (kg·s^{-1})	M	total reserve in the cold store (kg)
Q	cooling load (kW)	ΔQ	cooling load difference (kW)
i	input gate	EP	electricity price (CNY·kWh^{-1})
f	forgetting gate	COP	coefficient of performance
o	output gate	$COST$	total operation cost (CNY)
Subscripts			
is	isentropic	i	a certain moment
com	compressor	$1 \sim 4$	thermodynamic state point
eva	evaporator	ori	original (before optimization)
con	condenser	opti	optimized (after optimization)
high	the upper limit	dis	dissipation

References

1. Xu, Y.; Li, Z.; Chen, H.; Lv, S. Techno-economic evaluation and analysis of solar hybrid cooling systems with cool energy buffer for cold storages. *Sustain. Energy Technol. Assess.* **2021**, *46*, 101270. [CrossRef]
2. Shan, K.; Wang, J.; Hu, M.; Gao, D.-C. A model-based control strategy to recover cooling energy from thermal mass in commercial buildings. *Energy* **2019**, *172*, 958–967. [CrossRef]
3. Ding, Y.; Lyu, Y.; Lu, S.; Wang, R. Load shifting potential assessment of building thermal storage performance for building design. *Energy* **2022**, *243*, 123036. [CrossRef]
4. Belman-Flores, J.M.; Rodríguez-Valderrama, D.A.; Ledesma, S.; García-Pabón, J.J.; Hernández, D.; Pardo-Cely, D.M. A Review on Applications of Fuzzy Logic Control for Refrigeration Systems. *Appl. Sci.* **2022**, *12*, 1302. [CrossRef]
5. Comodi, G.; Carducci, F.; Nagarajan, B.; Romagnoli, A. Application of cold thermal energy storage (CTES) for building demand management in hot climates. *Appl. Therm. Eng.* **2016**, *103*, 1186–1195. [CrossRef]
6. Jin, X.; Zheng, S.; Huang, G.; Lai, A.C. Energy and economic performance of the heat pump integrated with latent heat thermal energy storage for peak demand shifting. *Appl. Therm. Eng.* **2023**, *218*, 119337. [CrossRef]
7. Sarafoji, P.; Mariappan, V.; Anish, R.; Karthikeyan, K.; Reddy, J. Performance study of solar photovoltaic cold storage system using phase change materials. *Mater. Today-Proc.* **2021**, *46*, 9623–9629. [CrossRef]
8. Saffari, M.; de Gracia, A.; Fernandez, C.; Belusko, M.; Boer, D.; Cabeza, L.F. Optimized demand side management (DSM) of peak electricity demand by coupling low temperature thermal energy storage (TES) and solar PV. *Appl. Energy* **2018**, *211*, 604–616. [CrossRef]
9. Arteconi, A.; Hewitt, N.J.; Polonara, F. State of the art of thermal storage for demand-side management. *Appl. Energy* **2012**, *93*, 371–389. [CrossRef]
10. Navidbakhsh, M.; Shirazi, A.; Sanaye, S. Four E analysis and multi-objective optimization of an ice storage system incorporating PCM as the partial cold storage for air-conditioning applications. *Appl. Therm. Eng.* **2013**, *58*, 30–41. [CrossRef]
11. Braun, J.E. Load Control Using Building Thermal Mass. *J. Sol. Energy Eng.* **2003**, *125*, 292–301. [CrossRef]
12. Verbeke, S.; Audenaert, A. Thermal inertia in buildings: A review of impacts across climate and building use. *Renew. Sustain. Energy Rev.* **2018**, *82*, 2300–2318. [CrossRef]
13. Shao, J.; Darkwa, J.; Kokogiannakis, G. Review of phase change emulsions (PCMEs) and their applications in HVAC systems. *Energy Build.* **2015**, *94*, 200–217. [CrossRef]
14. Mazzoni, S.; Sze, J.Y.; Nastasi, B.; Ooi, S.; Desideri, U.; Romagnoli, A. A techno-economic assessment on the adoption of latent heat thermal energy storage systems for district cooling optimal dispatch & operations. *Appl. Energy* **2021**, *289*, 116646. [CrossRef]
15. Gholamibozanjani, G.; Farid, M. Peak load shifting using a price-based control in PCM-enhanced buildings. *Sol. Energy* **2020**, *211*, 661–673. [CrossRef]
16. Bruno, F.; Tay, N.H.S.; Belusko, M. Minimising energy usage for domestic cooling with off-peak PCM storage. *Energy Build.* **2014**, *76*, 347–353. [CrossRef]
17. Rakkappan, S.R.; Sivan, S.; Ahmed, S.N.; Naarendharan, M.; Sai Sudhir, P. Preparation, characterisation and energy storage performance study on 1-Decanol-Expanded graphite composite PCM for air-conditioning cold storage system. *Int. J. Refrig.* **2021**, *123*, 91–101. [CrossRef]
18. Pirdavari, P.; Hossainpour, S. Numerical study of a Phase Change Material (PCM) embedded solar thermal energy operated cool store: A feasibility study. *Int. J. Refrig.* **2020**, *117*, 114–123. [CrossRef]

19. Bejarano, G.; Vargas, M.; Ortega, M.G.; Castaño, F.; Normey-Rico, J.E. Efficient simulation strategy for PCM-based cold-energy storage systems. *Appl. Therm. Eng.* **2018**, *139*, 419–431. [CrossRef]
20. Bista, S.; Hosseini, S.E.; Owens, E.; Phillips, G. Performance improvement and energy consumption reduction in refrigeration systems using phase change material (PCM). *Appl. Therm. Eng.* **2018**, *142*, 723–735. [CrossRef]
21. Hansen, E.; Lauridsen, L.; Skibsted, L.H.; Moawad, R.K.; Andersen, M.L. Oxidative stability of frozen pork patties: Effect of fluctuating temperature on lipid oxidation. *Meat Sci.* **2004**, *68*, 185–191. [CrossRef]
22. Teuteberg, V.; Kluth, I.K.; Ploetz, M.; Krischek, C. Effects of duration and temperature of frozen storage on the quality and food safety characteristics of pork after thawing and after storage under modified atmosphere. *Meat Sci.* **2021**, *174*, 108419. [CrossRef] [PubMed]
23. Akerma, M.; Hoang, H.-M.; Leducq, D.; Delahaye, A. Experimental characterization of demand response in a refrigerated cold room. *Int. J. Refrig.* **2020**, *113*, 256–265. [CrossRef]
24. Altwies, J.E.; Reindl, D.T. Passive thermal energy storage in refrigerated warehouses. *Int. J. Refrig.* **2002**, *25*, 149–157. [CrossRef]
25. Lv, Y.; Chu, Y.; Zhou, P.; Mei, J.; Xie, J. Effects of Different Freezing Methods on Water Distribution, Microstructure and Protein Properties of Cuttlefish during the Frozen Storage. *Appl. Sci.* **2021**, *11*, 6866. [CrossRef]
26. Mehling, H. Use of Phase Change Materials for Food Applications—State of the Art in 2022. *Appl. Sci.* **2023**, *13*, 3354. [CrossRef]
27. Yau, Y.H.; Lee, S.K. Feasibility study of an ice slurry-cooling coil for HVAC and R systems in a tropical building. *Appl. Energy* **2010**, *87*, 2699–2711. [CrossRef]
28. Yin, R.; Xu, P.; Piette, M.A.; Kiliccote, S. Study on Auto-DR and pre-cooling of commercial buildings with thermal mass in California. *Energy Build.* **2010**, *42*, 967–975. [CrossRef]
29. Lee, K.-H.; Braun, J.E. Model-based demand-limiting control of building thermal mass. *Build. Environ.* **2008**, *43*, 1633–1646. [CrossRef]
30. Sun, Y.; Wang, S.; Xiao, F.; Gao, D. Peak load shifting control using different cold thermal energy storage facilities in commercial buildings: A review. *Energy Convers. Manag.* **2013**, *71*, 101–114. [CrossRef]
31. Hinkelman, K.; Wang, J.; Zuo, W.; Gautier, A.; Wetter, M.; Fan, C.; Long, N. Modelica-based modeling and simulation of district cooling systems: A case study. *Appl. Energy* **2022**, *311*, 118654. [CrossRef]
32. Moffat, R.J. Describing the uncertainties in experimental results. *Exp. Therm. Fluid Sci.* **1988**, *1*, 3–17. [CrossRef]
33. Lu, Y.; Bai, T.; Yu, J. Experimental investigation on a −40 °C low-temperature freezer using ejector-expansion refrigeration system. *Int. J. Refrig.* **2020**, *118*, 230–237. [CrossRef]
34. Patil, R. Noise Reduction using Wavelet Transform and Singular Vector Decomposition. *Procedia Comput. Sci.* **2015**, *54*, 849–853. [CrossRef]
35. Hussain, T.; Deng, T.; Bradley, M.; Armour-Chélu, D.; Pillai, J.; Saadat, S.; Kaialy, W. Noise reduction by using wavelet transform in charge signal acquired from an electrostatic inductive sensor. *Meas. Sens.* **2023**, *27*, 100757. [CrossRef]
36. Li, Y.; Pan, X.; Liao, X.; Xing, Z. A data-driven energy management strategy based on performance prediction for cascade refrigeration systems. *Int. J. Refrig.* **2022**, *136*, 114–123. [CrossRef]
37. Bell, I.H.; Wronski, J.; Quoilin, S.; Lemort, V. Pure and Pseudo-pure Fluid Thermophysical Property Evaluation and the Open-Source Thermophysical Property Library CoolProp. *Ind. Eng. Chem. Res.* **2014**, *53*, 2498–2508. [CrossRef]
38. Hochreiter, S.; Schmidhuber, J. Long Short-Term Memory. *Neural Comput.* **1997**, *9*, 1735–1780. [CrossRef]
39. Yu, W. Empirical formulas for thermophysical properties calculation of Pork, Beef and Cod. *J. Dalian Fish. Univ.* **2000**, *2000*, 50–54. (In Chinese) [CrossRef]